Single-Fiber Lightwave Centralized WDM-OFDMA-PON with Colorless Optical Network Units

Siamak Amiralizadeh, An T. Nguyen, Chul Soo Park, and Leslie A. Rusch

Journal of Optical Communications and Networking, (Volume 8, Issue 4) (2015)

Doi: 10.1364/JOCN.8.000196

http://ieeexplore.ieee.org/document/7452818/

Single-Fiber Lightwave Centralized WDM-OFDMA-PON with Colorless Optical Network Units

Siamak Amiralizadeh, An T. Nguyen, Chul Soo Park, and Leslie A. Rusch

***Abstract*—We propose and experimentally demonstrate a carrier-reuse, single-feeder, wavelength-division-multiplexed, orthogonal-frequency-division-multiple-access passive optical network (WDM-OFDMA-PON) with colorless direct-detection optical network units and coherent detection optical line terminals. We examine two strategies by adjusting the frequency occupancy and the modulation format of the uplink (UL) and downlink (DL) signals. We investigate the impact of DL signal-to-carrier ratio on performance of both UL and DL via simulations and identify impairments limiting system performance. As a proof of concept, we demonstrate on a single wavelength channel, a realization of each of the two scenarios investigated using orthogonal-frequency-division-multiplexing (OFDM). A quadrature phase-shift keying approach with wide spectrum and narrow guard band achieves 21.6 Gb/s. A 32-ary quadrature amplitude modulation approach with narrow spectrum and wide guard band achieves 14.5 Gb/s and a span of over 80 km.**

***Index Terms*—Coherent detection, direct detection, optical fiber communication, orthogonal-frequency-division-multiplexing (OFDM), passive optical network (PON).**

I. Introduction

RESEARCH on future optical networks is driven by the growth in bandwidth-intensive applications and the requirement to accommodate data rates in Gb/s. Passive optical networks (PONs) are a promising solution for fiber-to-the-home due to their cost-efficiency and flexibility. Optimizing PON resources—a single fiber backbone and a distributed carrier being the most important—leads to even more cost-effective systems and decreases service provisioning expenses significantly [1]–[3].

Limitations in digital-to-analog/analog-to-digital converters (DACs/ADCs) would require excessive parallelization and processing for time-division-multiplexing (TDM)-PONs as bit rates scale up. Wavelength-division-multiplexing (WDM) has gained increased attention in the evolving PON standards process to accommodate the demand for high capacity [4]. Orthogonal-frequency-division-multiplexing (OFDM) is one option for future PONs, with the benefit of flexible bandwidth allocation and resilience in the face of chromatic dispersion. In orthogonal-frequency-division-multiple-access (OFDMA)-PONs, sub-bands of the total signal bandwidth can be allocated to optical network units (ONUs) rendering low cost ONUs. Thus, WDM-OFDMA-PON, combining the key advantages of the two strategies, is emerging as a promising solution [5]. All architectures demonstrated in [6]–[14] exploit direct-detection optical OFDM (DDO-OFDM) for downlink (DL) to minimize signal reception cost at ONU. In [6]–[10], the uplink (UL) is also directly detected at optical line terminal (OLT) receivers. This architecture allows a simple transceiver for both ONU and OLT, but leads to poor performance for the UL signal. Consequently, achieving symmetric bit rates is demanding, especially when resources are shared for the UL and DL.

Another approach is to use coherent detection for the UL signal transmission. Recently, a few PON architectures have been proposed deploying DDO-OFDM for DL and coherent optical OFDM (CO-OFDM) for UL [11]–[15]. The underlying reason for this combination is to reduce ONU implementation costs while taking advantage of superior performance for UL with a coherent receiver at OLT, and thus enabling symmetric data transmission rates. In [11], a high-capacity WDM-OFDMA-PON is demonstrated with separate fibers and sets of carriers for UL and DL in a remotely seeded fashion. Schindler *et al*. used a similar approach for UL and proposed an OFDMA-PON with a single feeder fiber and remote heterodyne reception for DL [12]. Implementation of the two architectures requires more components, although they are expected to have superior performance compared to lightwave centralized PONs using a single carrier for both UL and DL. In [13], the same carrier is used for the UL and DL while employing a guard band to avoid interference due to remodulation; however, the DL and UL signals are transmitted over two different fibers with 25 km length. Double feeder PONs are not cost-efficient, although they provide higher reach.

We demonstrate a symmetrical, single-feeder, lightwave centralized OFDMA-PON using an architecture similar to [14], [15]. In this PON architecture, one sideband of the signal spectrum is devoted to the DL signal while the other sideband is used for UL transmission. The proposed PON not only allows spectrally efficient signal transmission, but also enables us to use a single laser per WDM channel at the OLT for both DL and UL, enabling colorless ONUs. In [14], a single-fiber symmetrical 25 Gb/s OFDMA-POM is demonstrated with 20 km fiber length by using a single carrier for UL and DL. The main focus of [14] is power budget

Manuscript received November 12, 2015.

Siamak Amiralizadeh and Leslie A. Rusch are with the Center for Optics, Photonics, and Lasers (COPL), Electrical and Computer Engineering Department, Université Laval, Québec, QC G1V 0A6, Canada (e-mail: siamak.amiralizadeh-asi.1@ulaval.ca; rusch@gel.ulaval.ca).

An T. Nguyen and Chul Soo Park are with Infinera Corp., Sunnyvale, CA 94089, USA. (e-mail: anguyen@infinera.com; cpark@infinera.com).

discussions and resources allocation for UL and DL. In [15], the potential of the single carrier PON for achieving high UL data rate is experimentally demonstrated by using four WDM channels (32 Gb/s per channel) and real-time digital signal processing (DSP). Only UL transmission is demonstrated in [15].

In this paper, we concentrate on investigating the impairments that limit performance of the PON. We examine the impact of backscattering (BS) and particularly remodulation at ONU transmitter on performance of the UL and DL via analysis and Monte Carlo simulations. We demonstrate a proof-of-concept single WDM channel experiment with fiber length up to 80 km. We justify the results obtained in experiments by using the developed equations for the UL and DL signals. Our experiments and simulations study two scenarios for the frequency occupancy and the modulation format of the DL and UL signals. We discuss drawbacks and benefits of each scenario based on the analysis and the results obtained in simulations and experiments.

II. Lightwave Centralized WDM-OFDMA-PON Architecture

The key feature of the proposed carrier-reuse PON architecture is using DDO-OFDM for DL and CO-OFDM for UL, allowing a simple ONU transceiver and an OLT coherent detector. Single sideband (SSB) transmission of the OFDM signal is employed in the DL, and the other sideband is reserved for the UL to increase spectral efficiency. Figure 1 shows the WDM-OFDMA-PON architecture where w wavelength sources are used to generate multi-band OFDMA signals at the central office. The double sideband (DSB) OFDM signals are filtered to produce SSB OFDM. A guard band is introduced between the optical carrier and the DL signal. The guard band can be easily generated by inserting zero subcarriers in the OFDM signal before inverse fast Fourier transform (IFFT) at the transmitter. The SSB OLT signals are fed into an arrayed waveguide grating (AWG) to form a WDM transmission.

The signal is demultiplexed via an AWG after transmission over fiber. Each of the w OFDM signals is then split and distributed to a set of N ONUs. At each ONU, the received signal is split with a passive coupler; one portion of the signal is detected with a single photodiode (PD) and the other portion is remodulated with a reflective optical modulator unit. The UL signal is DSB with two symmetric sidebands. The UL signals from N ONUs are combined and transmitted over fiber after amplification at the ONU and multiplexing at the local exchange.

At the OLT, the received signal is demultiplexed. The sideband with heavy interference can be removed via filtering before detection. The UL OFDM signal is coherently detected via a local oscillator (LO) derived from the transmission source. The choice to filter the UL to SSB at the OLT instead of the ONU allows the ONU to remain colorless.

The proposed PON architecture employs OFDMA in combination with WDM to reach multiple users. In the simulations and experiments, we assume a single WDM channel with OFDM modulation and focus on investigating detrimental

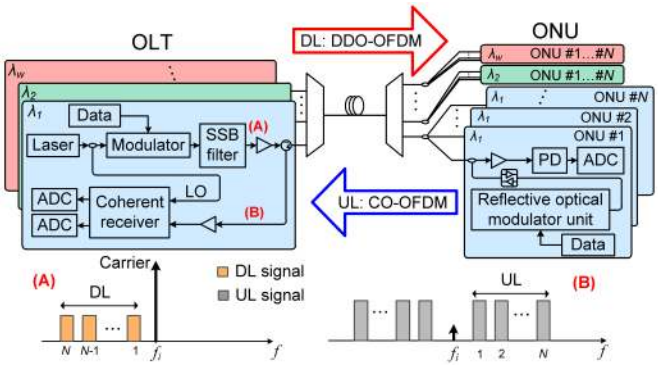

Fig. 1. Proposed carrier-reuse WDM-OFDMA-PON architecture with colorless direct detection ONU and coherent detection OLT.

PON impairments. The allocation of the resources to multiple users have been studied in previous demonstrations [14].

The main advantage of our proposed WDM-OFDMA-PON is optimally reusing the carrier and bandwidth. One of the major concerns in the carrier-reuse scheme is the residual DL signal that is remodulated with the carrier at the ONU modulator. The signal after the ONU modulator has two terms: 1) The UL signal generated by modulation of the carrier and 2) Interference due to remodulation of the DL signal by the UL signal. The second term can interfere with the detected sideband of the UL signal. The remodulation interference (RI) can be mitigated by properly choosing the DL and UL signal frequency bands with appropriate guard bands. Even if the two signals overlap in frequency on one sideband, as we will see in the next sections, the interference can be minimized by reducing the signal-to-carrier power ratio (SCR) of the DL signal. This leads to optical signal-to-noise ratio (OSNR) loss for the DL signal which is less critical in short-reach systems. BS is another important issue in single-feeder PONs. It originates from discrete components (e.g., connectors and couplers with limited directivity) or Rayleigh BS in the fiber [16].

In the next section, our main attention is on the impact of BS and RI on performance of the system assuming two different scenarios for the UL and DL signal. We use Monte Carlo simulations to justify our discussions and identify the influence of both RI and BS on the performance of each scenario.

III. PON Impairments

The two scenarios we examine are shown in Fig. 2. Both cases have symmetric UL and DL data rates, i.e., the same bandwidth and modulation format for UL and DL signals. In the first scenario, the gap between the SSB DL OFDM signal and the carrier is small. The UL signal has two sidebands with Hermitian symmetry and the left sideband is at the same frequency band as the DL signal (see the first two rows in Fig. 2 for case 1). In the second scenario, the gap between the SSB DL signal and the carrier is large enough to accommodate the UL signal bandwidth. The left sideband of the UL OFDM signal is located in the frequency band between the DL OFDM signal and the carrier without any overlap with the DL signal (see the first two rows in Fig. 2 for case 2).

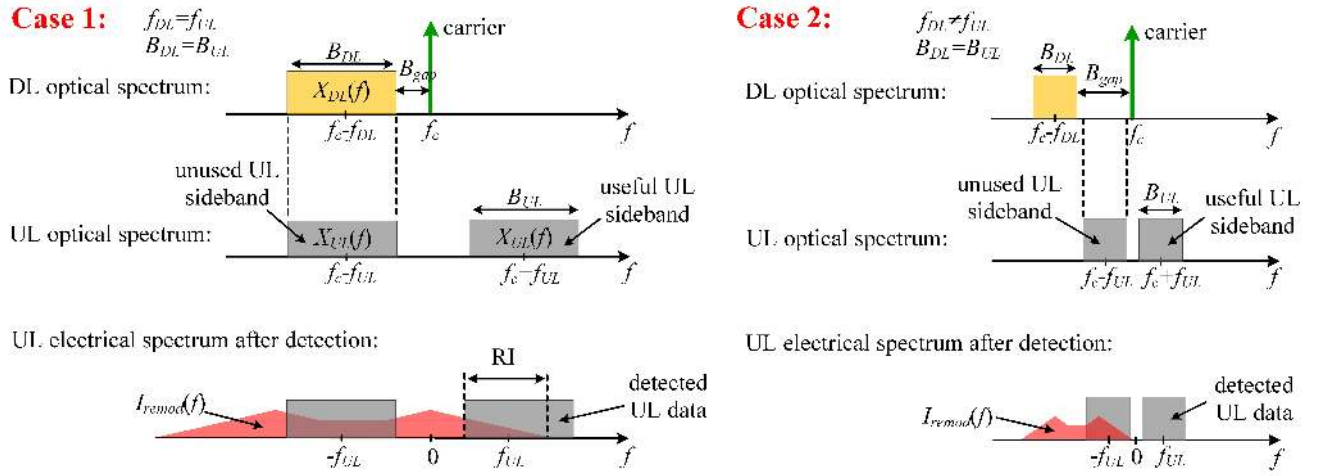

Fig. 2. Spectra of the DL and UL signal for the two scenarios in the simulations and experiments.

The first case uses the available bandwidth efficiently; however, it is more susceptible to the impairments. In the second case, the impairments are not as detrimental as the first case. Therefore, higher-order modulation formats can be used to compensate for inefficient bandwidth usage due to the larger guard band.

In the remainder of this section, we analyze the UL and DL signals in the PON and derive BS and remodulation terms. We employ the developed equations to identify the necessary condition for avoiding RI. We use Monte Carlo simulations to validate the analysis and demonstrate the impact of varying SCR on performance of the UL and DL.

A. System Model

Figure 3 depicts a block diagram of the lightwave centralized PON used for analysis and simulations. The signal after the SSB filter at the OLT consists of OFDM data and a carrier to directly detect the signal at the receiver. Let $E_{SSB}(t)$ be the DL signal after the SSB filter given by

$$E_{SSB}(t) = A_c \exp(j2\pi f_c t)\left[1+\gamma x_{DL}(t)\right], \tag{1}$$

where $x_{DL}(t)$ is the baseband SSB DL OFDM signal carrying data with normalized power, f_c is the optical carrier frequency, A_c is the amplitude of the optical carrier and γ^2 is the SCR. To focus on the impairments peculiar to the PON architecture (BS and RI), in the analysis we neglect any other noise and distortion in the system. The DL transmitted signal can be written as

$$E_{T,DL}(t) = \sqrt{\frac{P_{L,DL}}{P_{SSB}}} E_{SSB}(t), \tag{2}$$

where $P_{L,DL}$ is the DL launched power to the fiber and P_{SSB} is the power of the signal after the SSB filter. After transmission over the channel, the signal at the input of ONU reflective modulator is written as

$$E_{in,Mod}(t) = \sqrt{P_{R,DL}} E_{SSB}(t), \tag{3}$$

where

$$P_{R,DL} = \frac{P_{L,DL}}{2P_{SSB}} L_{fiber} G_{amp}, \tag{4}$$

L_{fiber} is the total fiber loss and G_{amp} is the amplifier gain. Assuming a linear optical modulator with power loss of L_{Mod} at the ONU transmitter, the modulator output signal, $E_{out,Mod}(t)$, can be written as

$$E_{out,Mod}(t) = \sqrt{L_{Mod}} x_{UL}(t) E_{in,Mod}(t), \tag{5}$$

where $x_{UL}(t)$ is the DSB UL electrical OFDM signal. By replacing Eq. (3) into Eq. (5) and using Eq. (1) we obtain

$$\begin{aligned} E_{out,Mod}(t) = {} & A_c \sqrt{L_{Mod} P_{R,DL}} \exp(j2\pi f_c t) x_{UL}(t) \\ & + E_{remod}(t), \end{aligned} \tag{6}$$

where

$$E_{remod}(t) = \gamma A_c \sqrt{L_{Mod} P_{R,DL}} x_{UL}(t) x_{DL}(t) \exp(j2\pi f_c t), \tag{7}$$

is the signal generated due to remodulation of the DL OFDM signal by the UL electrical OFDM signal. This remodulation term can interfere with the desired UL OFDM signal given by the first term in the right side of Eq. (6) and degrade UL performance.

The transmitted UL signal, $E_{T,UL}(t)$, can be expressed as

$$E_{T,UL}(t) = \sqrt{\frac{P_{L,UL}}{P_{R,DL} L_{Mod}}} E_{out,Mod}(t), \tag{8}$$

where $P_{L,UL}$ is the UL launched power. Both the received DL and UL signals are affected by the BS in the bidirectional PON. As a result, the received DL and UL signals are respectively given by

$$\begin{aligned} E_{R,DL}(t) = {} & \sqrt{P_{R,DL}} E_{SSB}(t) \\ & + \sqrt{2G_{amp}} \kappa_{UL} E_{T,UL}(t), \end{aligned} \tag{9}$$

and

$$\begin{aligned} E_{R,UL}(t) = {} & \sqrt{L_{fiber} G_{amp}} E_{T,UL}(t) \\ & + \sqrt{G_{amp}} \kappa_{DL} E_{T,DL}(t), \end{aligned} \tag{10}$$

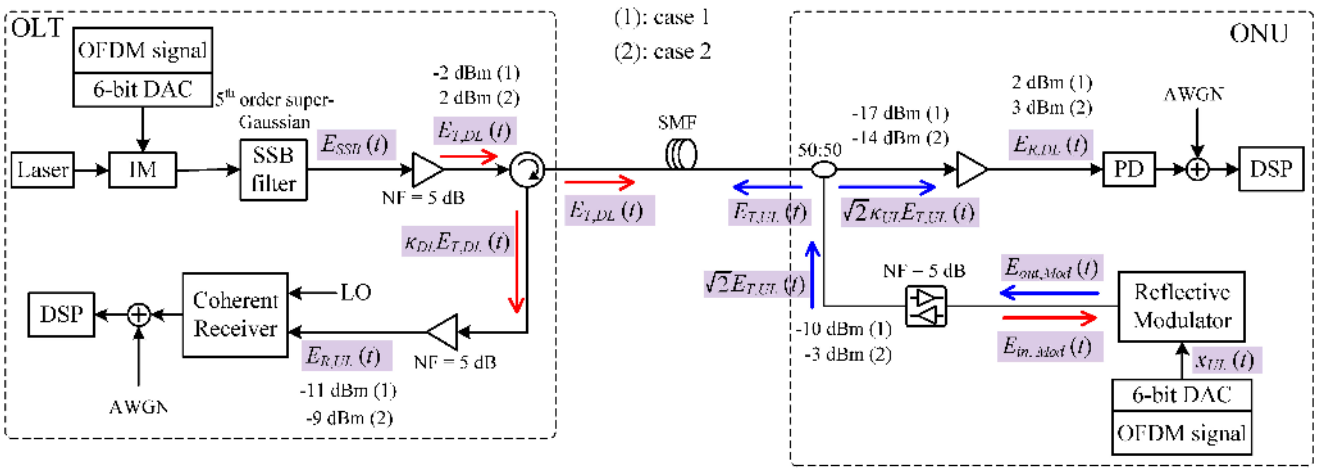

Fig. 3. Block diagram of simulator with terms from analytic equations shown in shaded text. Powers are indicated at various junctures for each of the two cases studied.

where κ_{UL} and κ_{DL} are the BS coefficients of the UL and DL signals, respectively. The BS coefficients determine the power of the signal in the backward direction.

After direct detection by a square-law PD at the ONU receiver, removing the direct current (DC) term and simplifying, the detected DL signal can be written as

$$\begin{aligned} r_{DL}(t) &= |E_{R,DL}(t)|^2 \\ &= 2\gamma P_{R,DL}|A_c|^2\Re\{x_{DL}(t)\} \\ &+ \gamma^2 P_{R,DL}|A_c|^2|x_{DL}(t)|^2 \\ &+ c_1|E_{SSB}(t)|^2 x_{UL}(t) \\ &+ 2G_{amp}\kappa_{UL}^2|E_{T,UL}(t)|^2, \end{aligned} \tag{11}$$

where

$$c_1 = 2\kappa_{UL}G_{amp}\sqrt{\frac{P_{L,UL}P_{L,DL}L_{fiber}}{P_{SSB}}}. \tag{12}$$

The first term in Eq. (11) is the desired DL OFDM signal and the second term is the well-known signal-signal beat interference (SSBI) due to direct detection [17]. The third and fourth terms exist due to BS in the PON. Since the BS coefficient is small in practice, the fourth term can be neglected. Simplification of the third term gives the BS signal, $r_{BS,DL}(t)$, after PD as

$$\begin{aligned} r_{BS,DL}(t) \approx |A_c|^2 c_1 x_{UL}(t) + |A_c|^2 c_1\gamma^2|x_{DL}|^2 x_{UL}(t) \\ + 2|A_c|^2 c_1\gamma\Re\{x_{DL}(t)\}x_{UL}(t). \end{aligned} \tag{13}$$

In Eq. (13), the first term has only the UL signal, $x_{UL}(t)$. Therefore, for the first scenario where UL and DL have the same frequency band, this term induces interference to the DL signal. However, the first term does not interfere with the DL signal in the second scenario since UL and DL use different frequency bands. The second and third terms in Eq. (13) induce interference to the DL signal in both scenarios.

For the UL, by replacing Eq. (2) and Eq. (8) into Eq. (10) and using Eq. (1) and Eq. (6) the signal after coherent detection can be obtained as

$$\begin{aligned} r_{UL}(t) &= c_2 x_{UL}(t) + i_{remod}(t) \\ &+ \gamma\kappa_{DL}A_c A_{LO}\sqrt{\frac{P_{L,DL}G_{amp}}{P_{SSB}}}x_{DL}(t), \end{aligned} \tag{14}$$

where

$$c_2 = A_c A_{LO}\sqrt{P_{L,UL}G_{amp}L_{fiber}}, \tag{15}$$

A_{LO} is the LO amplitude, and

$$i_{remod}(t) = c_2\gamma x_{DL}(t)x_{UL}(t) \tag{16}$$

is the RI. As illustrated in the third row of Fig. 2, the remodulation term shown by triangular (red color) spectra does not interfere with the detected sideband of the UL signal (upper-frequency sideband) in the second scenario. However, it induces interference to the UL signal in the first scenario. By taking the Fourier transform of $i_{remod}(t)$ and comparing its frequency band to the frequency band of the UL signal, it is straightforward to obtain the condition for preventing interference to the UL signal as

$$B_{UL} \leq B_{gap}, \tag{17}$$

where B_{UL} is bandwidth of the UL OFDM signal and B_{gap} is bandwidth of the guard band (gap) between the DL signal and the carrier. This condition is met in the second case. Thus, the remodulation term does not induce any degradation to the signal in this case.

The third term in the right side of Eq. (14) is the BS induced to the UL signal. The backscattered signal and the detected UL signal are at different sidebands. Therefore, contrary to DL, BS does not degrade UL signal performance.

B. Simulations

We turn to simulations to validate our predictions for the two scenarios. In the simulations, the IFFT size is 256. Eight samples are added to each OFDM symbol as a cyclic prefix to enable efficient channel equalization at the receiver. In the first scenario, a quadrature phase-shift keying (QPSK) DL signal

occupies a frequency band from 2 GHz to 13 GHz at the left side of the carrier. The DSB QPSK UL signal occupies the frequency bands at both sides of the carrier. Each of the DL and UL signal has 100 data-bearing subcarriers.

In the second scenario, a 32-ary quadrature amplitude modulation (32-QAM) DL signal has a bandwidth from 4.8 GHz to 7.9 GHz and the UL signal has a bandwidth from 0.65 GHz to 3.9 GHz on both sides of the carrier. Each of the DL and UL signals has 28 data subcarriers. The bit rate is 21.6 Gb/s for the first scenario and 14.5 Gb/s for the second scenario.

Two pre-emphasized pilot subcarriers are inserted in the UL OFDM signal for phase noise compensation (50^{th} and 80^{th} subcarrier for the first case and 20^{th} and 30^{th} subcarrier for the second case). The DAC is modeled as a 6-bit quantizer with 13 GHz analog bandwidth and 28 GS/s sampling rate. In our experiments, limited effective number of bits (ENOB) for the DAC was the main limiting factor in achieving higher bit rates for the second scenario, which is not modeled in the simulations. Therefore, it would be possible to obtain the same bit rate for the first and second case in the simulations. However, we simulate the more realistic situation where bit rates would vary due to DAC impairments. The bit rates simulated reflect those we were able to achieve in our proof-of-concept experiments.

The laser source at the OLT with 10 kHz linewidth is modulated by an ideal intensity modulator (IM). A fifth-order super-Gaussian filter is used to remove one sideband of the DL OFDM signal. Single-mode fiber (SMF) is modeled as a linear medium with dispersion parameter of 16 ps/nm·km. The amplifiers have a noise figure (NF) of 5 dB. The ONU receiver is a square-law detector and the OLT coherent receiver uses a 10 kHz laser as LO. The transmitted and received powers are given in Fig. 3 for both cases. The powers are adjusted according to our experimental setup described in section IV. Thermal noise-limited reception is assumed with -13 dBm and -24 dBm additive white Gaussian noise (AWGN) power for the DL and UL receiver, respectively. The BS coefficients are $\kappa_{UL} = \kappa_{DL} = -42$ dB, as measured in the experiments.

Figure 4(a) shows DL bit error rate (BER) versus DL SCR for the two cases. For the first case, SSBI given by the second term in Eq. (11) degrades performance of the DL when SCR is high. As we decrease SCR, the SSBI decreases leading to a better BER. Further decreasing SCR from the optimum value of -16 dB increases BER due to the BS and the amplifier noise. From Eq. (11), we know that the desired DL OFDM signal is proportional to $\gamma|A_c|^2$. On the other hand, the first term in the BS signal given by Eq. (13) depends on carrier power, $|A_c|^2$. Therefore, as γ (or SCR) decreases, the ratio between desired DL OFDM signal and BS signal decreases resulting in performance degradation.

For the second scenario, the SSBI does not degrade the DL OFDM signal performance [17]; we observe a BER floor at high SCR due to DL receiver noise. As discussed before, the first term of the BS signal does not interfere with the DL signal in this case. Therefore, the main limitation at low SCR is due to the amplifier noise. BER results without BS is also shown in Fig. 4(a) to confirm our discussions. We observe that BS has negligible effect on BER in the second case; however, it has considerable impact on BER in the first case.

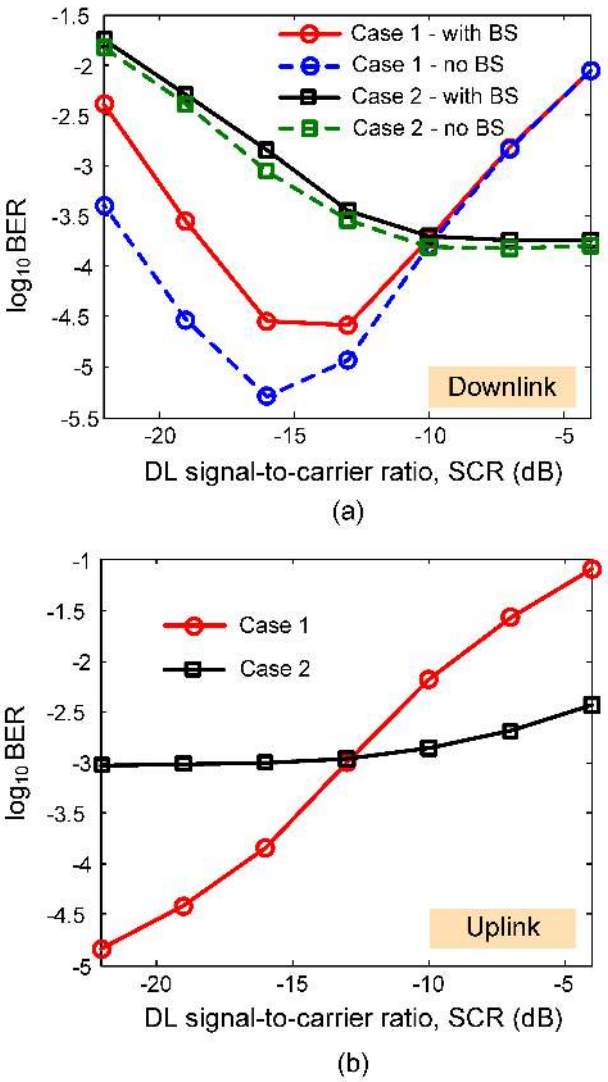

Fig. 4. BER simulation results versus DL SCR for the two scenarios. (a) DL, (b) UL with BS.

Figure 4(b) shows BER of UL signal versus DL SCR. The RI given by Eq. (16) increases as DL SCR increases. Since the first case does not respect the condition given in Eq. (17), RI induces significant degradation to the UL signal as SCR increases. We observe slight performance degradation for the second case by increasing SCR. Increasing DL SCR decreases power of the carrier available for UL remodulation. This power decrease in the useful portion of the UL OFDM signal leads to OSNR loss and degrades signal performance; however, the degradation is not significant as compared to the first case.

IV. Experimental Setup and Spectral Effects

Figure 5 depicts the experimental setup for single channel PON with OFDM. As a reflective Mach-Zehnder modulator (MZM) is unavailable, we replace the reflective optical modulator unit of Fig. 1 with non-reflective MZM and an optical circulator. At both OLT and ONU transmitters, independent QAM OFDM signals are generated using pseudo

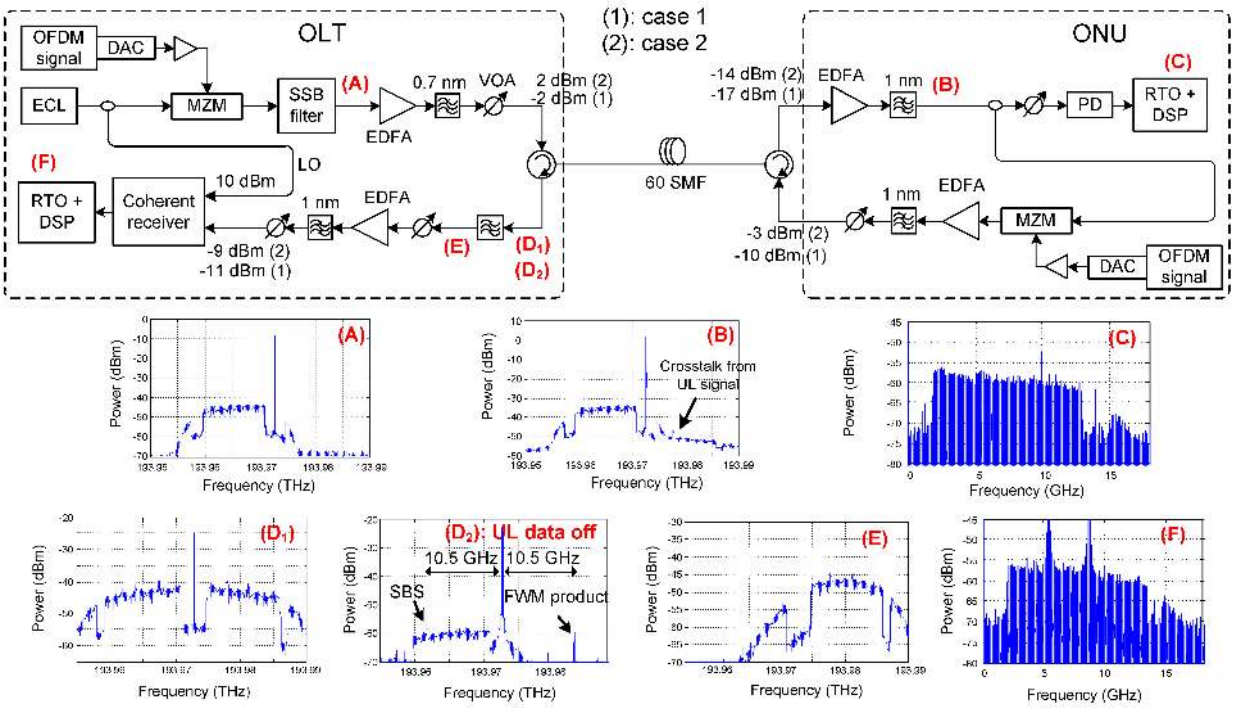

Fig. 5. Experimental setup for single channel OFDMA-PON. Inset: signal spectra at 0.8 pm (100 MHz) resolution.

random binary sequences (PRBSs) with the length of $2^{21}-1$. The parameters used for OFDM signals are similar to our simulations presented in section III-B. After taking IFFT and adding cyclic prefix in Matlab, the generated signals are loaded into memory of two field programmable gate arrays (FPGAs) and then converted into analog signals using DACs with 6 bits resolution operating at 28 GS/s. The electrical OFDM signals from DACs are amplified and drive two MZMs (Fujitsu FTM7937EZ-A and FTM7938EZ), one for ONU and one for OLT. At the OLT, an external cavity laser (ECL) at 1546.62 nm with 10 kHz linewidth is modulated by an MZM biased at quadrature. To decrease the power fading effect, an optical SSB filter (Yenista XTM-50) rejects one OFDM sideband (see Fig. 5A). The signal power is adjusted to -2 dBm for the first case and 2 dBm for the second case with a variable optical attenuator (VOA) after amplification via erbium-doped fiber amplifier (EDFA).

The OFDM signal is launched into standard SMF. We assume splitting loss at the ONU can be compensated for with the ONU optical amplifier. The ONU received signal is split (3-dB coupler) with one output detected by a PD (u2t XPDV3120R), and the other output fed into a $LiNbO_3$ MZM biased at the null point after manually adjusting the polarization. The UL OFDM signal is then amplified and launched back into the channel. The UL launched power is -10 dBm and -3 dBm for the first and second case, respectively. Note that the VOAs are not required for the PON implementation; they are used to control the signal power. Furthermore, while we use EDFAs due to limitation in the available components, application of SOAs are preferred in the ONU because of their cost-effectiveness, integrability and wide spectral gain. At the OLT receiver, the lower sideband of the OFDM signals is filtered with a tunable optical filter (see Fig. 5D_1 and E) and then coherently detected with an LO. The detected signals at both ONU and OLT are digitized using a real-time oscilloscope (RTO) and processed offline. The spectrum of the received signal for ONU and OLT is shown in Fig. 5C and F, respectively.

We note that while employing the SSB filter before the coherent receiver improves receiver sensitivity, when removing the filter we can still obtain acceptable performance given that the coherent receiver input power is increased and the carrier is suppressed effectively at ONU modulator. We also note that the MZMs used in our experiment are polarization sensitive; however, they can be replaced by polarization-independent reflective MZMs [18].

Figure 5B shows the spectrum of the DL OFDM signal after transmission; this is remodulated at the ONU transmitter. There is crosstalk induced by the DSB UL signal to the DL signal. Note that we avoid using an SSB filter at the ONU transmitter to have a simple colorless ONU. The observed crosstalk is mostly due to limited directivity of the optical circulator ($\sim$ 42 dB) and partly because of BS from discrete components and Rayleigh BS. We categorize all of these effects as BS. We used low launched power at the ONU to minimize DL signal performance degradation. However, when using a reflective optical modulator, limited directivity of the coupler at ONU (rather than optical circulator) can lead to crosstalk. Couplers with directivity of as high as 55 dB are commercially available, providing 13 dB more protection than our experimental demonstration. In our experiments, we show that even in the worst case scenario when the UL and DL signals use the same frequency range at two sides of the carrier (first case) BER below forward error correction (FEC)

threshold of 3.8×10^{-3} (7% overhead) can be achieved.

Figure 5D$_2$, taken at the OLT receiver after the circulator, shows the impact of stimulated Brillouin scattering (SBS) on the UL signal. We turned off the electrical UL OFDM data to highlight the SBS effect from the DL signal. SBS is caused by the $\chi^{(3)}$ nonlinearity in the fiber and occurs at slightly lower frequencies than the incident light in the backward direction. Since the high-frequency sideband is used for the UL signal transmission, SBS from the DL signal is not at the same sideband as the UL signal. However, due to presence of the SBS tone and the carrier in the UL direction, they interact with each other through four-wave mixing (FWM) phenomenon and create a third tone at the high-frequency sideband (see Fig. 5D$_2$). The FWM product of the carrier and SBS occurs at ~ 10.5 GHz spacing from the carrier. As we will see in section V-A, the distortion from FWM product affects only a few subcarriers (two in our case). Hence, it is not a major problem in the proposed PON and can be easily avoided by properly designing the subcarrier structure for the UL signal.

V. Experimental Results

A. First Case: QPSK Experiment

Figure 6(a) depicts BER versus received power for 21.6 Gb/s bidirectional QPSK OFDM signal which corresponds to the first scenario as described in the previous sections. The received power is measured before PD for the DL and before the EDFA at the OLT receiver for the UL. The SCR of the DL signal is -17 dBm. For the DL signal, performance is limited due to receiver noise. The PD used does not have a transimpedance amplifier (TIA) and the receiver sensitivity is low compared to previous PON demonstrations with direct detection for DL [8]. This limitation is not related to the architecture of the PON and can be alleviated by employing a commercially available PD-TIA with high sensitivity at the ONU.

The UL signal has superior performance compared to the DL signal due to coherent detection. BER is below the FEC limit of 3.8×10^{-3} for the swept received power range. As we showed in the simulations, decreasing DL SCR decreases RI in UL. By using low SCR for the DL signal (-17 dBm), the RI in the UL is reduced in the experiments. We also show the DL signal BER results when the UL data is turned off to see the impact of BS. We observed 0.5 dB power penalty at BER equal to FEC threshold of 3.8×10^{-3}. Lower BER floor is achieved when BS is eliminated by turning off the UL data. This confirms our observation in simulations for DL signal for the first case.

In Fig. 6(b), error vector magnitude (EVM) versus subcarrier index is shown for the UL and DL signal with 60 km SMF. All subcarriers achieve EVM less than the FEC limit. We notice that two subcarriers (at ~ 10.5 GHz) suffer distortion coming from FWM of the carrier and SBS in the UL. Although the induced distortion is not severe due to low launched power to the fiber, it can be avoided entirely by considering a few null subcarriers at the Brillouin frequency shift. The SBS nonlinear effect is observed at relatively low powers—the threshold for SBS is approximately 2 dBm [19]. Hence, the launched power per channel must be below the threshold power to avoid significant power saturation and attenuation due to SBS.

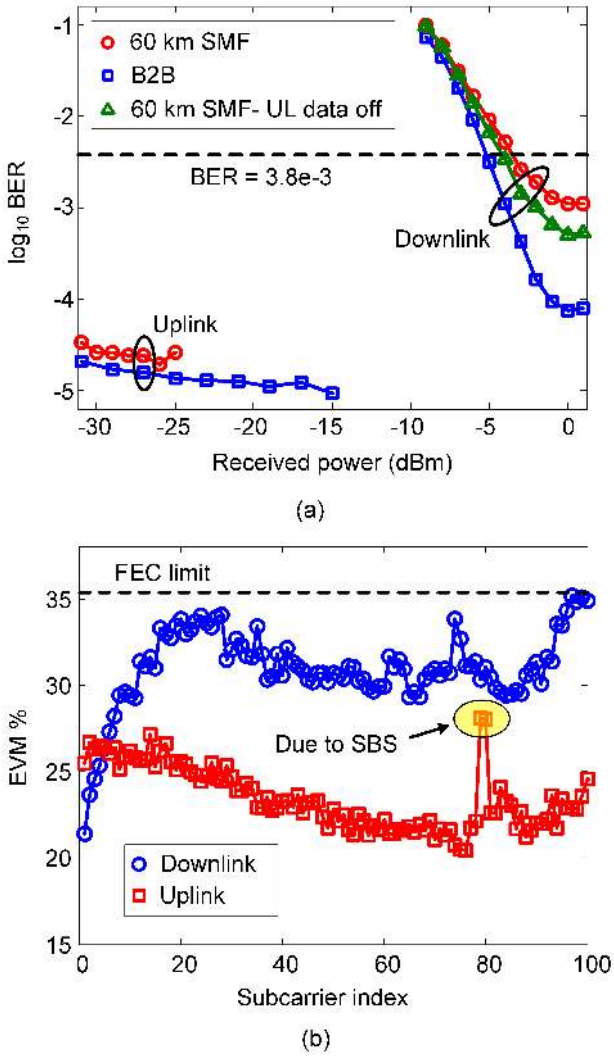

Fig. 6. Experimental results for 21.6 Gb/s bidirectional QPSK OFDM. (a) BER versus received power. (b) EVM versus subcarrier index for the DL and UL signal with 60 km SMF.

B. Second Case: 32-QAM Experiment

Figure 7 shows BER versus fiber length for 32-QAM OFDM signal. We were able to increase the launched power for the DL and UL signal to 2 dBm and -3 dBm, respectively, since the second case is less vulnerable to RI and BS as discussed in section III. The power at the input of DL PD and UL coherent receiver is 3 dBm and -9 dBm, respectively. The results show that system reach can be extended to 80 km in the second case achieving BER below hard-decision FEC limit of 3.8×10^{-3}.

For the DL, the observed performance degradation when increasing fiber length is due to increased BS interference from the UL signal to the DL signal. As Eq. (11) indicates, by increasing the fiber length the desired DL OFDM signal given by the first term of Eq. (11) decreases by a factor of L_{fiber}. As the UL and DL launched power is kept constant, the BS signal given by Eq. (13) decreases by a factor of $\sqrt{L_{fiber}}$.

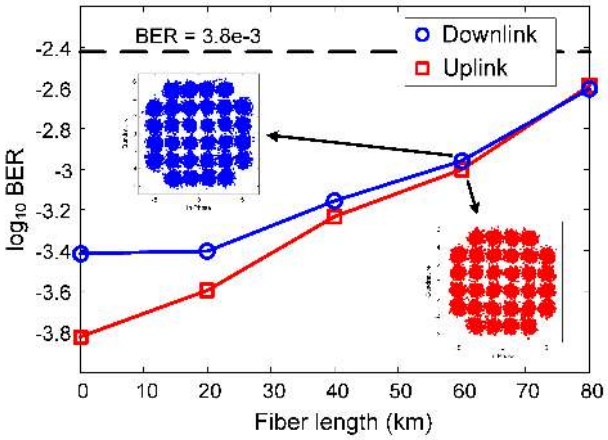

Fig. 7. BER versus fiber length for 14.5 Gb/s bidirectional 32-QAM OFDMA-PON.

Therefore, the ratio between the desired DL signal and the BS decreases by increasing fiber length. Since we use direct detection at the DL receiver, BS still induces interference, although it is less severe in this case where the DL and UL do not share frequency bands [20]. In the UL, BS does not lead to performance degradation due to coherent detection as we discussed in section III. However, as we extend the fiber length the input power to the optical modulator at the ONU decreases leading to OSNR loss for the UL signal.

VI. Conclusion

We demonstrated a single-fiber lightwave centralized WDM-OFDMA-PON. Our proposed architecture uses DDO-OFDM for DL to minimize ONU implementation cost. We use CO-OFDM for UL to enable symmetric data transmission rates despite the signal quality degradation on the UL when using remodulation. We analyzed the impairments peculiar to the PON architecture and validated our discussions with simulations. We showed that RI can be detrimental for the UL and identified the necessary condition for preventing RI. This condition is respected in the second case. We minimized the RI by decreasing DL SCR in the first case where this condition is not respected. For the DL, BS is one of the main limiting factors in the first scenario where UL and DL signals overlap in frequency. BS has negligible impact on the performance in the second scenario. Experiments show that BER below FEC threshold can be achieved for both DL and UL even in the worst case where the UL and DL signals completely overlap in frequency. This suggests the UL signal performance is not a bottleneck in the proposed PON architecture. We demonstrate 21.6 Gb/s bidirectional QPSK OFDMA-PON over 60 km of SMF. We show that system reach can be extended to 80 km for 14.5 Gb/s 32-QAM with different frequency bands for the DL and UL.

Acknowledgments

This work was supported by TELUS and NSERC under CRD grant 437041.

References

[1] N. Cvijetic, "OFDM for next-generation optical access networks," *J. Lightw. Technol.*, vol. 30, no. 4, pp. 384–398, Feb. 2012.

[2] E. Wong, "Next-generation broadband access networks and technologies," *J. Lightw. Technol.*, vol. 30, no. 4, pp. 597–608, Feb. 2012.

[3] P. Vetter, "Next generation optical access technologies," presented at the Eur. Conf. on Opt. Commun., Amsterdam, The Netherlands, 2012, paper Tu.3.G.1.

[4] P. Prat, "Technologies for a cost effective UDWDM-PON," presented at the Opt. Fiber Commun. Conf., Los Angeles, CA, USA, 2015, paper Th3I.3.

[5] J. von Hoyningen-Huene and C. Ruprecht, "OFDM for optical access," presented at the Opt. Fiber Commun. Conf., Los Angeles, CA, USA, 2015, paper Tu1H.1.

[6] H.-Y. Chen, M. Yuang, P.-L. Tien, D.-Z. Hsu, C.-C. Wei, Y.-S. Tsai, and J. Chen, "Design and demonstration of a colorless WDM-OFDMA PON system architecture achieving symmetric 20-Gb/s transmissions with residual interference compensation," *Opt. Express*, vol. 21, no. 18, pp. 21097–21104, 2013.

[7] E. Hugues-Salas, R. P. Giddings, X. Q. Jin, Y. Hong, T. Quinlan, S. Walker, and J. M. Tang, "REAM intensity modulator-enabled 10Gb/s colorless upstream transmission of real-time optical OFDM signals in a single-fiber-based bidirectional PON architecture," *Opt. Express*, vol. 20, no. 19, pp. 21089–21100, 2012.

[8] T. Dong, Y. Bao, Y. Ji, A. P. T. Lau, Z. Li, and C. Lu, "Bidirectional hybrid OFDM-WDM-PON system for 40-Gb/s downlink and 10-Gb/s uplink transmission using RSOA remodulation," *IEEE Photon. Technol. Lett.*, vol. 24, no. 22, pp. 2024–2026, Nov. 2012.

[9] J. Yu, M.-F. Huang, D. Qian, L. Chen, and G.-K. Chang, "Centralized lightwave WDM-PON employing 16-QAM intensity modulated OFDM downstream and OOK modulated upstream signals," *IEEE Photon. Technol. Lett.*, vol. 20, no. 18, pp. 1545–1547, Sep. 2008.

[10] I. N. Cano, X. Escayola, P. C. Schindler, M. C. Santos, V. Polo, J. Leuthold, I. Tomkos, and J. Prat, "Experimental demonstration of a statistical OFDM-PON with multiband ONUs and elastic bandwidth allocation," *J. Opt. Commun. Netw.*, vol. 7, no. 1, pp. A73–A79, 2015.

[11] N. Cvijetic, M. Cvijetic, M.-F. Huang, E. Ip, Y.-K. Huang, and T. Wang, "Terabit optical access networks based on WDM-OFDMA-PON," *J. Lightw. Technol.*, vol. 30, no. 4, pp. 493–503, Feb. 2012.

[12] P. C. Schindler, R. Schmogrow, M. Dreschmann, J. Meyer, I. Tomkos, J. Prat, H.-G. Krimmel, T. Pfeiffer, P. Kourtessis, A. Ludwig, D. Karnick, D. Hillerkuss, J. Becker, C. Koos, W. Freude, and J. Leuthold, "Colorless FDMA-PON with flexible bandwidth allocation and colorless, low-speed ONUs," *J. Opt. Commun. Netw.*, vol. 5, no. 10, pp. A204–A212, 2013.

[13] M.-F. Huang, D. Qian, and N. Cvijetic, "A novel symmetric lightwave centralized WDM-OFDM-PON architecture with OFDM-remodulated ONUs and a coherent receiver OLT," presented at the Eur. Conf. on Opt. Commun., Geneva, Switzerland, 2011, paper Tu.5.C.1.

[14] A. Lebreton, B. Charbonnier, and J. Le Masson, "A single wavelength 25-Gb/s symmetric FDMA PON," *J. Lightw. Technol.*, vol. 33, no. 8, pp. 1630–1634, Apr. 2015.

[15] S. Straullu, P. Savio, A. Nespola, J. Chang, V. Ferrero, R. Gaudino, and S. Abrate, "Demonstration of upstream WDM+FDMA PON and real time implementation on an FPGA platform," presented at the Eur. Conf. Opt. Commun., Valencia, Spain, 2015, paper Mo.3.4.3.

[16] P. Gysel and R. K. Staubli, "Statistical properties of Rayleigh backscattering in single-mode fibers," *J. Lightw. Technol.*, vol. 8, no. 4, pp. 561–567, Apr. 1990.

[17] A. J. Lowery and J. Armstrong, "Orthogonal-frequency-division multiplexing for dispersion compensation of long-haul optical systems," *Opt. Express*, vol. 14, no. 6, pp. 2079–2084, 2006.

[18] B. Charbonnier, N. Brochier, and P. Chanclou, "Reflective polarisation independent Mach-Zenhder modulator for FDMA/OFDMA PON," *Electron. Lett.*, vol. 46, no. 25, pp. 1682–1683, 2010.

[19] J. Toulouse, "Optical nonlinearities in fibers: review, recent examples, and systems applications," *J. Lightw. Technol.*, vol. 23, no. 11, pp. 3625–3641, Nov. 2005.

[20] C. W. Chow, C. H. Yeh, C. H. Wang, F. Y. Shih, and S. Chi, "Rayleigh backscattering performance of OFDM-QAM in carrier distributed passive optical networks," *IEEE Photon. Technol. Lett.*, vol. 20, no. 18, pp. 1545–1547, Sep. 2008.

Siamak Amiralizadeh (S'12) was born in Tabriz, Iran, in 1989. He received the B.S. degree in electrical engineering from Sharif University of Technology, Tehran, Iran in 2011 and the M.S. degree in electrical engineering from the Center for Optics Photonics, and Lasers (COPL), ECE department, Université Laval, QC, Canada, in 2014, where he is currently working towards the Ph.D. degree. His current research interests include advanced modulation formats, digital signal processing for high-speed optical transmission, and optical networks. He has served as a reviewer for *Optics Express*, *IEEE Journal of Lightwave Technology*, *IEEE Photonics Technology Letters*, *Optica*, and *Optics Communications*.

An T. Nguyen was born in 1982. He received the B.S. degree in physics in 2003 and M.S. degree in electronics engineering in 2007 from University of Science—Vietnam National University (VNU) in Ho Chi Minh City, Vietnam. From 2003 to 2007, he stayed at VNU as a research assistant working on WirelessLAN and WirelessMAN physical layer, mainly on forward error coding, channel modeling and channel estimation. From 2008 to 2011, he was pursuing his Ph.D. degree in optical telecommunications at the Centro di Eccellenza per l'Ingegneria dell'Informazione, della Comunicazione e della Percezione (CEIICP) of Scuola Superioré Sant'Anna, Pisa, Italy. His research topics involved ultra-fast (640 Gbps and beyond) OTDM subsystems, multifunctional hybrid add/drop node for OTDM and WDM integration, all-optical wavelength and modulation format converter, ultrafast packet switching and photonic digital processing circuits. From 2012 to 2015, he was with the Center for Optics, Photonics, and Lasers (COPL), Université Laval, Québec, Canada. His projects focus on optical coherent detection systems with higher-order modulation formats, OFDM-over-fiber and full-duplex wireless-fiber interfacing. He is currently with Infinera Corp., Sunnyvale, CA, USA.

Chul Soo Park Chul Soo Park received the B.S. degree from the Kwangwoon University, Seoul, Korea in 1997 and the M.S. and Ph.D. degree from the Gwangju Institute of Science and Technology (GIST), Gwangju, Korea, in 1999, and 2006, respectively. In 2005, He was a part-time research staff in the Korea Photonics Technology Institute (KOPTI) where he developed the visible light communication link and related free-space communication transceivers. From 2006 to 2012, he was a research scientist at Institute for Infocomm Research (I2R), A*STAR, Singapore. He was co-principal investigator of 60-GHz microwave photonic system research collaborated with NICT, Japan, and worked on optoelectronic circuit development for ONFIG-II project. Also he was a main contributor for 60GHz high speed Ethernet video streaming using photonic technology in Fusion Light project. He served as an executive committee member for IEEE Singapore Section during 2010 and 2011 and publication chair for the international topical meeting on microwave photonics 2011 (MWP2011). From 2012 to 2015, he worked for Center for Optics, Photonics, and Lasers (COPL), Université Laval, Canada, as a senior researcher/laboratory manager where he worked on optical coherent detection system and silicon photonics device research. He is currently with Infinera Corp., Sunnyvale, CA, USA.

Leslie A. Rusch (S'91-M'94-SM'00-F'10) received the B.S.E.E. degree (with honors) from the California Institute of Technology, Pasadena, in 1980 and the M.A. and Ph.D. degrees in electrical engineering from Princeton University, Princeton, NJ, in 1992 and 1994, respectively. Dr. Rusch has experience in defense, industrial and academic communications research. She was a communications project engineer for the Department of Defense from 1980-1990. While on leave from Université Laval, she spent two years (2001-2002) at Intel Corporation creating and managing a group researching new wireless technologies. She is currently a Professor in the Department of Electrical and Computer Engineering at Université Laval, QC, Canada, performing research on wireless and optical communications. She is a member of the Centre for Optics, Photonics, and Lasers (COPL) at Université Laval. Prof. Rusch's research interests include digital signal processing for coherent detection in optical communications, spatial multiplexing using orbital angular momentum modes in fiber, radio over fiber and OFDM for passive optical networks; and in wireless communications, optimization of the optical/wireless interface in emerging cloud based computing networks, optical pulse shaping for high-bit rate ultrawide-band (UWB) systems, and implantable medical sensors with high bit rate UWB telemetry. She is recipient of the IEEE Canada J. M. Ham Award for Graduate Supervision. Prof. Rusch has published over 100 journal articles in international journals (90% IEEE/IEE) with wide readership, and contributed to over 140 conferences. Her articles have been cited over 4000 times per Google Scholar.